PPPL--2393

DE87 003071

Impurity Transport in Ohmic- and Neutral-Beam-Heated TFTR Discharges

B. C. Stratton, S. A. Cohen, F. P. Boody, C. E. Bush*, R. Ellis III, R. J. Fonck, E. Fredrickson, B. Grek, R. J. Groebner**, K. W. Hill, R. A. Hulse, D. Johnson, B. LeBlanc, E. S. Marmar***, K. McGuire, D. McNeill, A. T. Ramsey, J. F. Schivell, S. Sesnic, and J. Timberlake

Princeton University, Plasma Physics Laboratory, Princeton, NJ 08544

*Oak Ridge National Laboratory, Oak Ridge, TN 37831

**GA Technologies, Inc., San Diego, CA 92138

***Francis Bitter National Magnet Laboratory, Massachusetts Institute of Technology, Cambridge, MA 02139

Abstract

Impurity transport has been studied in ohmic- and neutral-beam-heated TFTR discharges by observation and numerical modeling of time evolutions of emissions from germanium injected using the laser-blowoff method. VUV spectral lines, the total radiated power, and soft x-ray intensities are compared with code predictions in which the impurity flux is assumed to have diffusive and convective terms. In plasmas with I_p=1.4 MA and $\bar{n}_e \approx 2.5 \times 10^{13}$ cm^{-3}, little difference in transport between ohmic and beam-heated discharges is observed. At I_p=0.7 MA and $\bar{n}_e \approx 1.0 \times 10^{13}$ cm^{-3}, a three-fold increase in the diffusion coefficient is found during beam heating.

Presented at the Plasma-Surface Interactions Conference, Princeton, 5-9 May 1986. To be published in Journal of Nuclear Materials

1. Introduction

The effects of impurities on tokamak plasmas depend on the quantity and distribution of the impurities in the plasma, which are determined by impurity transport processes as well as impurity sources. This paper presents the initial results of impurity transport experiments in ohmic- and neutral-beam-heated Tokamak Fusion Test Reactor (TFTR) plasmas.

2. Measurements and Modeling

An impurity transport code is used to model the time evolution of emissions from germanium injected into the plasma by the laser-blowoff technique [1]. Similar studies have been performed on a number of tokamaks [2]. The laser-blowoff method of impurity injection is described in detail elsewhere [3-5]. Germanium (Z=32) was chosen because it is not fully ionized at the central electron temperature ($T_e(0)$=2-5 keV) of the discharges under study. Germanium was injected during the steady-state phase of the discharge, and two VUV spectrographs, SPRED [6] (λ>100 Å) and SOXMOS [7] (λ<100 Å), were used to observe the time evolutions of the intensities of the following lines: Ge XIV 112.9 Å, Ge XV 117.3 Å, Ge XXI 196.6 Å, Ge XXII 226.5 Å, and Ge XXIX 92.8 Å. Transport code calculations show that for the plasmas considered here the fractional abundances of these ionization states peak at locations spanning the entire plasma radius, from r=75 cm for GeXIV to r=0 cm for Ge XXIX. The plasma was limited by a graphite blade limiter located on the large major radius side of the torus; the major and minor radii were 82 cm and 255 cm, respectively. The spectrograph detector integration time, which determines the time resolution of the measurements, was 3.3 ms for SPRED and 50 ms for SOXMOS. (The longer integration time used by SOXMOS was adequate to observe the relatively slow time evolution of the Ge XXIX line.) The time evolution of the total radiated power was measured using a wide-angle bolometer system (10 ms time resolution) and the time behavior of the soft x-ray (1-5 keV) emissions was observed using an array of silicon-diode detectors with sub-millisecond time resolution.

The MIST (Multi-Ionic Species Transport) code [8] was used to model the data. The code is one-dimensional: impurity distributions are assumed to be poloidally and toroidally symmetric inside the limiter radius. MIST solves the set of coupled equations

$$\frac{\partial n_q}{\partial t} = -\frac{1}{r}\frac{\partial (r\Gamma_q)}{\partial r} + I_{q-1}n_{q-1} - (I_q + R_q)n_q + R_{q+1}n_{q+1} - n_q/\tau_q + S_q. \quad (1)$$

The index q, indicating the ionization state, runs from zero to Z, the nuclear charge of the element. Γ_q is the impurity flux density, n_q is the impurity density, I_q is the ionization rate, R_q is the recombination rate, τ_q is a confinement time describing parallel loss to the limiter of ions in the scrape-off region, and S_q describes the impurity source and recycling. The recombination rates include charge-exchange processes due to beam and thermal neutrals, in addition to radiative and dielectronic processes. T_e and n_e profiles measured by Thomson scattering immediately before injection are input into the code. The T_e and n_e profiles in the scrape-off region are characterized by decay lengths obtained from probe measurements [9] in similar TFTR discharges. The injection process can strongly perturb the plasma edge; complications arising from such perturbations are ignored in this preliminary analysis and will be studied in detail later.

The impurity flux density is taken to have the form

$$\Gamma_q = -D\frac{\partial n_q(r)}{\partial r} + v_q n_q(r). \quad (2)$$

For simplicity, impurity transport is assumed to be independent of ionization state. D is a diffusion coefficient assumed to be constant as a function of radius. The convective velocity is parameterized in one of two ways:

$$v(r) = -c_1\,(2D/a)(r/a), \text{ or} \quad (3)$$

$$v(r) = c_2\, D\,\frac{\partial \ln[n_e(r)]}{\partial r}, \quad (4)$$

where a is the minor radius of the plasma and c_1 and c_2 are constants. In equilibrium ($\Sigma\,\Gamma_q$=0 for r≤a), assumed for intrinsic impurity analysis, the shape of the total impurity density $n_z(r)=\Sigma\, n_q(r)$ is determined by $v(r)/D$. Because D is assumed constant, v(r) determines the shape of $n_z(r)$. If equation 3 is used, the equilibrium $n_z(r)$ has the form of a Gaussian to the power c_1; if equation 4 is used, $n_z(r)$ has the shape of $n_e(r)$ to the power c_2 [10,11]. Both parameterizations were used in order to test the sensitivity of the results to the chosen form. Both forms yield a v(r) that is zero on axis and has its maximum at the plasma edge.

Equation 4 with c_2=1 predicts equilibrium impurity concentrations that are constant as a function of radius. The flat Z_{eff} profiles within r< 60 cm measured on TFTR [12] imply that intrinsic impurity (primarily carbon and oxygen) concentrations are independent of radius. Also, equilibrium MIST modeling of brightnesses of intrinsic nickel, chromium, and iron lines indicates that the concentrations of these impurities are constant as a function of radius [12]. It is therefore of interest in these initial studies to consider models of the injected germanium data using equation 4 with c_2 approximately equal to one.

The impurity source is assumed to be instantaneous and recycling is zero; the neutral germanium atoms are ionized near the limiter radius. The scrape-off layer confinement time is assumed to be the same for all ionization states and is parameterized by a scale length λ_{so} according to $\tau_q=\lambda_{so}^2/D$. λ_{so} represents the effective distance outside the limiter radius of the particle sink.

The brightnesses of the observed lines and total radiated power as a function of time are calculated from the radial distribution of the ionization states obtained from solution of equations 1. D, c_1 or c_2, and λ_{so} represent a three-parameter transport model and are adjusted to give the best qualitative fit to the data. Because the ionization rates are poorly known for germanium, their values were varied over a limited range (a factor of 0.5 or 2.0) around their nominal values [8]. The calculations are insensitive to similar variations in the recombination rates.

3 Transport in an Ohmically Heated Discharge

To provide a point of reference for comparison with other cases and to check the sensitivity of the results to the values of parameters assumed in the model, transport in ohmically heated plasmas with I_p=1.4 MA, B_t=4.0 T, $\bar{n}_e$=2.5 X 10^{13} cm^{-3}, and $T_e(0)$=2.2 keV was studied in detail. The data were obtained in a series of identical discharges. The global impurity confinement time measured from the late part of the decay of the GeXXIX line brightness, the total radiated power, and the soft x-ray signal was ~0.22 sec [1].

Sawteeth were present on the soft x-ray emissions and on $T_e(0)$ from electron-cyclotron emission measurements. Sawteeth were included in the transport model in a simple way by flattening the total impurity density within a chosen mixing radius at the time of each sawtooth [13]. The T_e and n_e profiles were not changed. The mixing radius was chosen to be 1.4 times the radius of the q=1 surface [14], 27 cm in this case.

The time evolutions of the germanium emissions were first modeled with D=1.0 X 10^4 cm^2/sec, a convective velocity given by equation 3 with c_1=0.3, and λ_{s0}=25 cm. The measured and calculated time evolutions of the Ge XIV and Ge XXIX lines and the total radiated power are shown in Figs. 1 and 2. The calculated and measured intensities were normalized at the peak values. Because MIST does not calculate soft x-ray emissivities, the soft x-ray data were modeled using the time evolution of the total germanium density on axis for the decay time and the same quantity at 30 cm for the rise time (Fig. 3). The soft x-ray signal is a line average measurement; this procedure accounts for the variation in the time behavior of the emissivity with radius in an approximate way. (Sawteeth do not appear on the Ge XXIX line brightness because the detector integration time was comparable to the sawtooth period.) The peaking parameter c_1=0.3 corresponds to a convective velocity at the limiter radius of approximately 75 cm/sec. Similar agreement between the calculations and data was also obtained using a convective velocity parameterized according to equation 4 with c_2=0.3.

A reasonable fit to the data was also obtained using $D=1.0 \times 10^4$ cm^2/sec, $c_1=1.0$, $\lambda_{so}=5$ cm, and a multiplier on all the ionization rates of 0.5. A similar fit was obtained with $c_2=0.75$ in equation 4, consistent with the intrinsic impurity results previously mentioned. Either of these parameterizations of the convective velocity is equivalent to a convective velocity of approximately 225 cm/sec at the limiter radius.

The value of the convective velocity is not well determined in the present analysis since, by varying the values of λ_{so} and the ionization rate multiplier, good fits to the data can be obtained with different values of the convective velocity. However, a nonzero inward convective velocity with a value of 75-225 cm/sec at the limiter radius gives the best fit to the present data. Less sensitivity is seen in the determination of the diffusion coefficient, with different models yielding approximately 1.0×10^4 cm^2/sec. It is probable that a radially varying diffusion coefficient and/or a parameterization of the convective velocity different from equations 3 and 4 could give equally good fits to the data, and such possibilities are presently under study. The relative intensities of the lines could provide another constraint on the diffusion coefficient and the convective velocity. The above models did not yield a good fit to the relative intensities of all the lines. A possible explanation is that the calculated brightnesses of lines emitted by high ionization states, such as Ge XXIX, are quite sensitive to the ionization rates.

4. Comparison of Transport in Beam- and Ohmically Heated Discharges

Figure 4 shows the time evolution of the Ge XXIX line for injection into the neutral-beam-heated period of a discharge with $I_p=1.4$ MA and $\overline{n}_e=2.2 \times 10^{13}$ cm^{-3}. The duration of the 3.5 MW beam pulse was 0.5 sec, and germanium was injected 0.2 sec into the pulse. Also shown in Fig. 5 is the time evolution of the Ge XXIX line from injection of the same quantity of germanium into the ohmic period, 0.4 sec after the end of the beam pulse, of a similar discharge with $I_p=1.4$ MA, $\overline{n}_e=2.5 \times 10^{13}$ cm^{-3}, and 3.8

MW beam power. The rise and decay times of the signals are similar to each other and to those in the ohmic discharge discussed in the preceding section. This is also true for the other germanium lines, and the peak intensities of the lines are the same for injection during the beam pulse and after it. (Because beam injection caused a significant rise in the soft x-ray emission and radiated power in this case, it was not possible to measure accurately the rise and decay times of these signals.) Thus, there appears to be no dramatic difference in the transport in beam-heated and ohmic discharges at I_p=1.4 MA and $\overline{n}_e$=2.5 X 10^{13} cm^{-3}.

In the energetic-ion regime [15], I_p=0.7 MA and $\overline{n}_e \approx 1.0 \times 10^{13}$ cm^{-3}, there is a difference in the time evolution of the emissions from the same amount of germanium injected into the beam pulse and into the ohmic period of the discharge. This is seen most clearly in the soft x-ray signal from a detector with a chord height of 20 cm above the plasma midplane shown in Fig. 5 for injection 0.2 sec into a 4.6 MW beam pulse and into the ohmic period, 0.4 sec after the end of the beam pulse, of a similar discharge. The rise and decay times and peak intensity of the signal are smaller by approximately a factor of three for injection into the beam pulse compared to injection into the ohmic period of the discharge. The soft x-ray data can be used in this case because the background decreases with beam injection. The rise and decay times of the Ge XXI and Ge XXII line brightnesses are shorter by a factor of approximately two for injection into the beam pulse, but have the same peak values as for injection into the ohmic period of the discharge. The brightness of the Ge XXIX line was too small for its rise and decay time to be reliably measured. The rise and early part of the decay of the total radiated power and its peak value are the same for injection into the beam pulse and into the ohmic period of the discharge. Because the signal is weak later in time, it is not possible to measure accurately the decay time. These observations show that the global confinement time of germanium injected into the beam pulse is shorter than for injection into the ohmic period of the discharge.

These differences in the rise and decay times are fit by $D \approx 3.0 \times 10^4$ cm^2/sec for injection into the beam pulse and $D \approx 1.0 \times 10^4$ cm^2/sec for injection into the ohmic period of the discharge. A convective velocity parameterized by c_1=1.0 in equation 3 and λ_{s0}=5 cm was used. It was not possible to fit the differences in the data by keeping $D \approx 1.0 \times 10^4$ cm^2/sec and λ_{s0}=5 cm and changing the magnitude or direction of the convective velocity.

The toroidal rotation velocity of the plasma during the beam pulse measured by the Doppler shift of the Ti XXI K_α line was large, approximately 5×10^7 cm/sec [15]. Burrell *et al.* [16] and Stacey *et al.* [17] have proposed modifications to neoclassical impurity transport theory which predict that impurities could be expelled from plasmas having large toroidal rotation velocities. However, it is not clear that the effects of rotation are seen in the present data.

5. Summary

Impurity transport in ohmic- and beam-heated TFTR discharges has been studied by MIST impurity transport code modeling of emissions from germanium injected using the laser-blowoff technique. For ohmic- and beam-heated plasmas with I_p=1.4 MA and $\bar{n}_e \approx 2.5 \times 10^{13}$ cm^{-3}, preliminary modeling of the transport indicates $D \approx 1.0 \times 10^4$ cm^2/sec and $v(a) \approx 75-225$ cm/sec. Similar transport is found during the ohmic period of discharges with I_p=0.7 MA and $\bar{n}_e \approx 1.0 \times 10^{13}$ cm^{-3}. However, during beam heating in these discharges (energetic-ion regime), the situation is considerably different: the decay times of the signals decrease by a factor of 2-3, indicating that $D \approx 3.0 \times 10^4$ cm^2/sec. Work is in progress to model accurately the relative intensities of the lines and the time evolutions of the lines emitted by some of the charge states. Further work will consider spatially varying diffusion coefficients, the effects of plasma rotation, a more sophisticated sawtooth model, and edge perturbations due to the injection process itself.

Acknowledgments

We would like to thank R. Goldston, D. Grove, R. Hawryluk, D. Meade, J. D. Strachan, K. Young, and the TFTR operating physicists for their support of this work. This work was supported by U. S. DoE contract no. DE-AC02-76-CHO-3073.

References

[1] J. Timberlake, S. A. Cohen, F. P. Boody *et al.*, Bull. Am. Phys. Soc. 30 (1985) 1522.

[2] For a review, see R. C. Isler, Nucl. Fusion 24 (1984) 1599.

[3] E. S. Marmar, J. L. Cecchi, and S. A. Cohen, Rev. Sci. Instrum. 46 (1975) 1149.

[4] D. Manos, D. Ruzic, R. Moore *et al.*, J. Vac. Sci. Technol. 20 (1982) 1230.

[5] S. Cohen, J. Cecchi, C. Daughney *et al.*, J. Vac. Sci. Technol. 20 (1982) 1226.

[6] R. J. Fonck, A. T. Ramsey, and R. V. Yelle, Appl. Opt. 21 (1982) 2115.

[7] J. L. Schwob, M. Finkenthal, S. Suckewer, in Vacuum Ultraviolet Radiation Physics, VUV VII, (Proceedings of the 7th International Conference, Jerusalem, 1983).

[8] R. A. Hulse, Nucl. Technol./Fusion 3 (1983) 259.

[9] S. J. Kilpatrick, D. M. Manos, R. V. Budny *et al.*, J. Vac. Sci. Technol. A 4 (1986) 1817.

[10] R. A. Hulse, in Princeton Plasma Physics Lab. Report PPPL-2182, edited by C. E. Singer (1985).

[11] R. J. Fonck and R. A. Hulse, Phys. Rev. Lett. 52 (1984) 530.

[12] B. C. Stratton, F. P. Boody, R. J. Fonck *et al.*, Bull. Am. Phys. Soc. 30 (1985) 1387.

[13] K. Ida, R. J. Fonck, R. A. Hulse, and B. LeBlanc, Plasma Phys. and Cont. Fusion 28 (1986) 879.

[14] B. B. Kadomtsev, Sov. J. Plasma Phys. 1 (1975) 389.

[15] M. Murakami, V. Arunasalam, J. D. Bell *et al.*, Plasma Phys. and Cont. Fusion 28 (1986) 17.

[16] K. H. Burrell, T. Ohkawa, and S. K. Wong, Phys. Rev. Lett. 47 (1981) 511.

[17] W. M. Stacey, Jr., R. B. Bennett, and D. J. Sigmar, J. Nucl. Mat. 121 (1984) 82.

Figure Captions

1. Measured (solid line) and calculated (dashed line) time evolutions of Ge XIV and Ge XXIX line brightnesses for germanium injection into an ohmic discharge with I_p=1.4 MA and $\bar{n}_e$=2.5 X 10^{13} cm^{-3}.

2. Measured (solid line) and calculated (dashed line) total radiated power for the plasma conditions of Fig. 1.

3. Measured (solid line) central-chord soft x-ray signal for the plasma conditions of Fig. 1 and calculated total germanium density (dashed lines) at r=0 cm and r=30 cm for the same conditions.

4. Time evolution of Ge XXIX line brightness for germanium injection into ohmic- and beam-heated discharges at I_p=1.4 MA and $\bar{n}_e \approx$2.5 X 10^{13} cm^{-3}.

5. Soft x-ray signals (chord height=20 cm) for germanium injection into ohmic- and beam-heated discharges at I_p=0.7 MA and $\bar{n}_e \approx$1.0 X 10^{13} cm^{-3}.

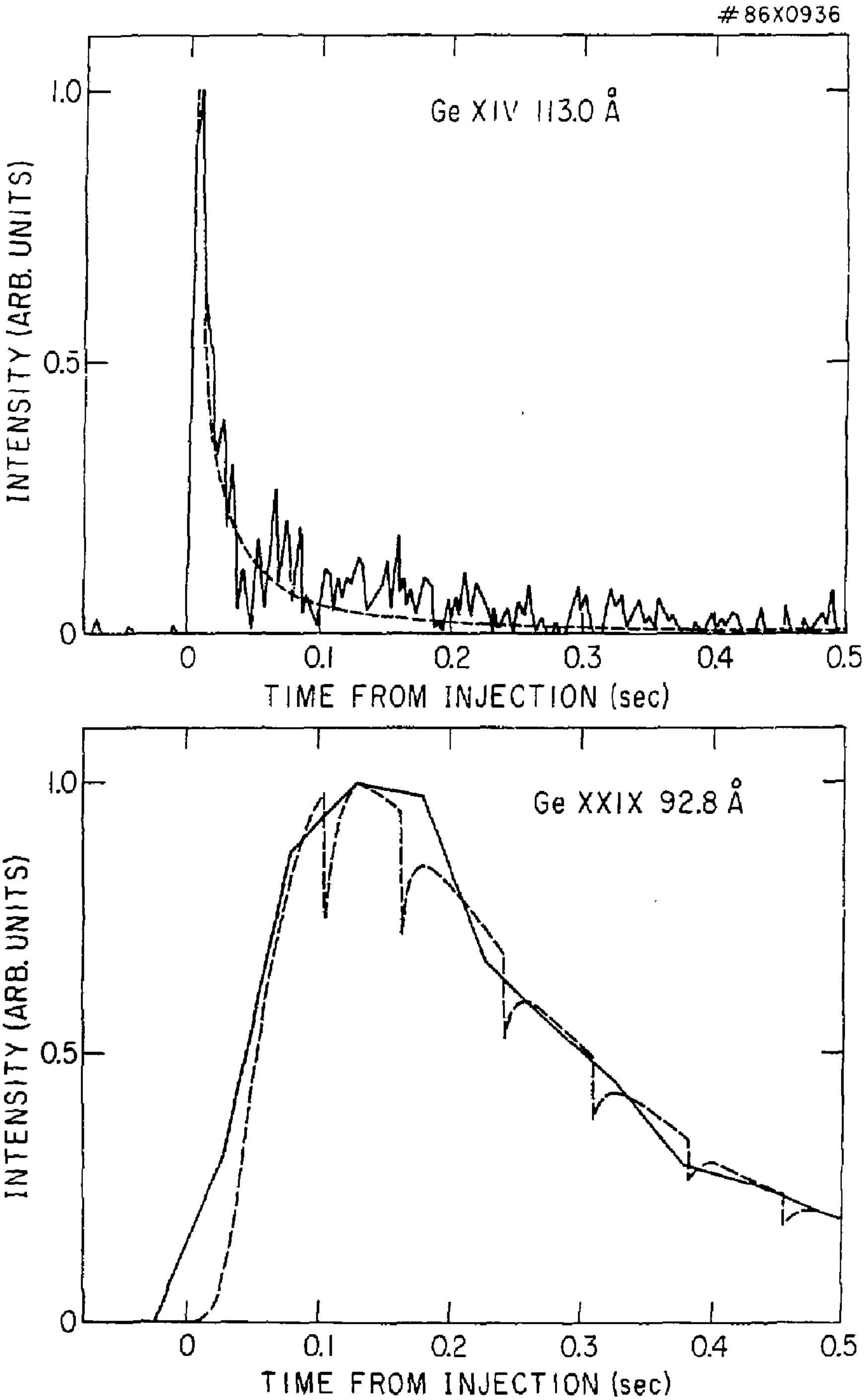

#86X0936
Ge XIV 113.0 Å
INTENSITY (ARB. UNITS)
1.0
0.5
0
0
0.1
0.2
0.3
0.4
0.5
TIME FROM INJECTION (sec)
Ge XXIX 92.8 Å
INTENSITY (ARB. UNITS)
1.0
0.5
0
0
0.1
0.2
0.3
0.4
0.5
TIME FROM INJECTION (sec)

Fig. 1

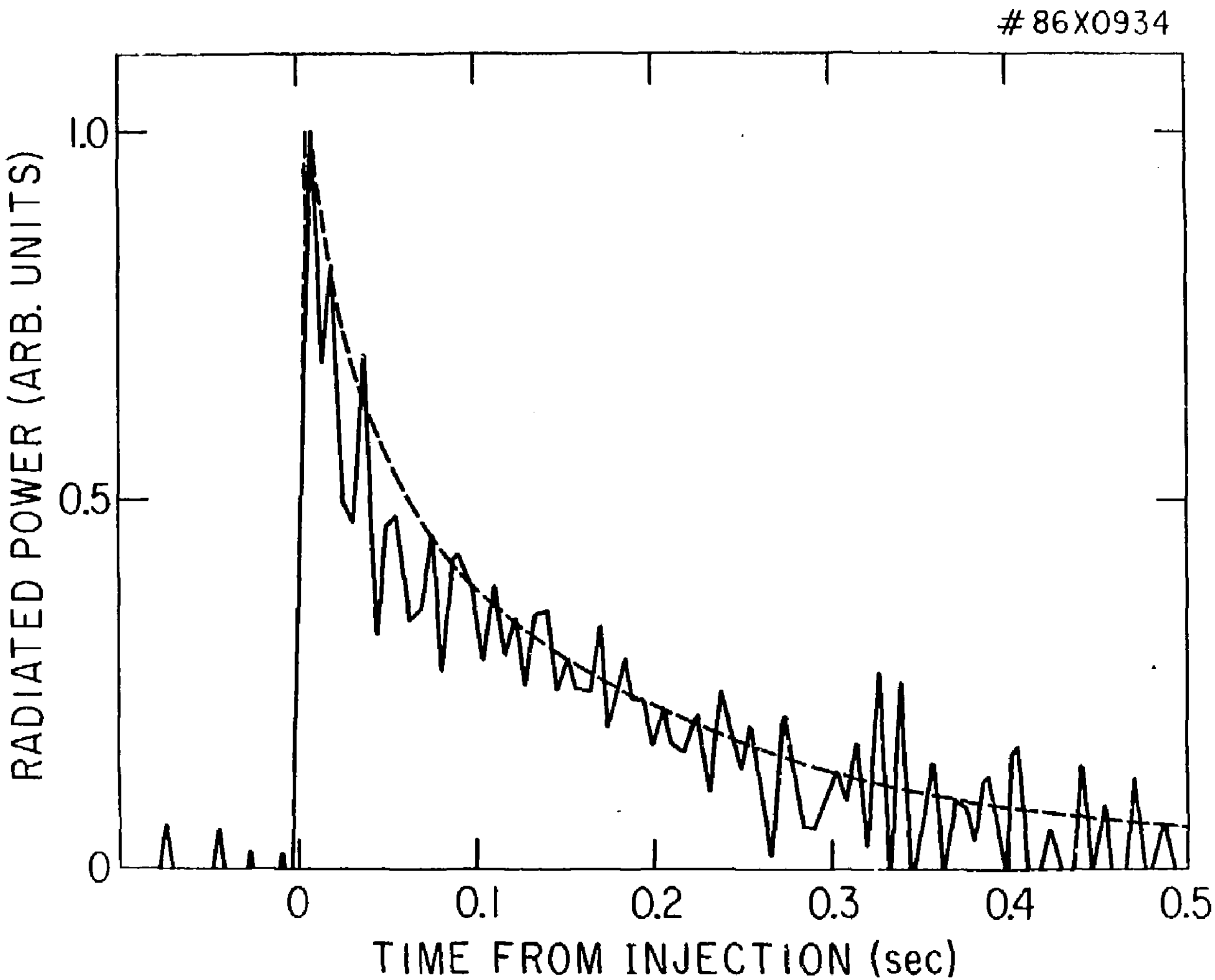

#86X0934
1.0
0.5
0
RADIATED POWER (ARB. UNITS)
0
0.1
0.2
0.3
0.4
0.5
TIME FROM INJECTION (sec)

Fig. 2

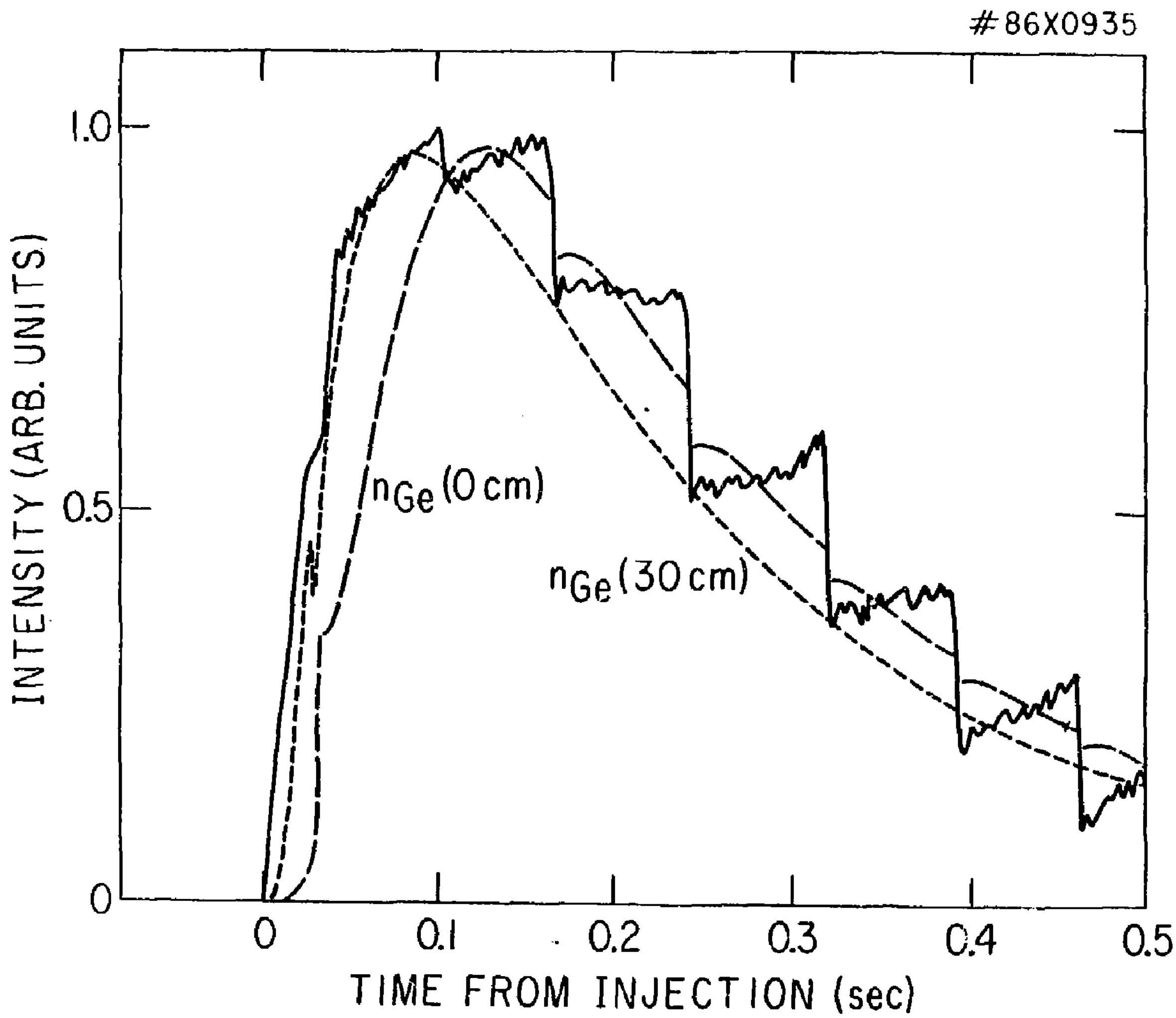
#86X0935
INTENSITY (ARB. UNITS)
1.0
0.5
0
n_{Ge}(0 cm)
n_{Ge}(30 cm)
0
0.1
0.2
0.3
0.4
0.5
TIME FROM INJECTION (sec)

Fig. 3

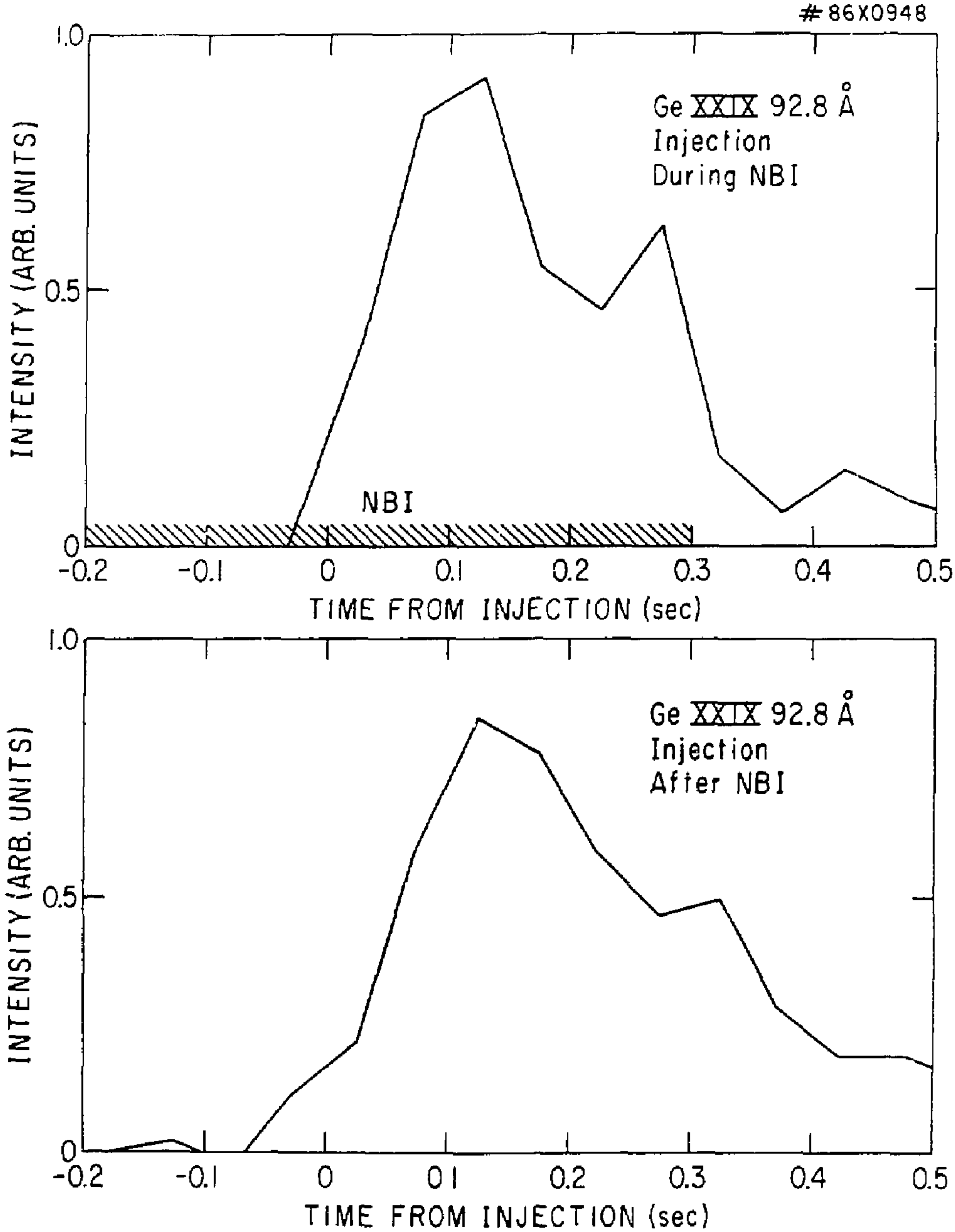

86X0948
1.0
0.5
0
INTENSITY (ARB. UNITS)
Ge XXIX 92.8 Å
Injection
During NBI
NBI
-0.2
-0.1
0
0.1
0.2
0.3
0.4
0.5
TIME FROM INJECTION (sec)
1.0
0.5
0
INTENSITY (ARB. UNITS)
Ge XXIX 92.8 Å
Injection
After NBI
-0.2
-0.1
0
0.1
0.2
0.3
0.4
0.5
TIME FROM INJECTION (sec)

Fig. 4

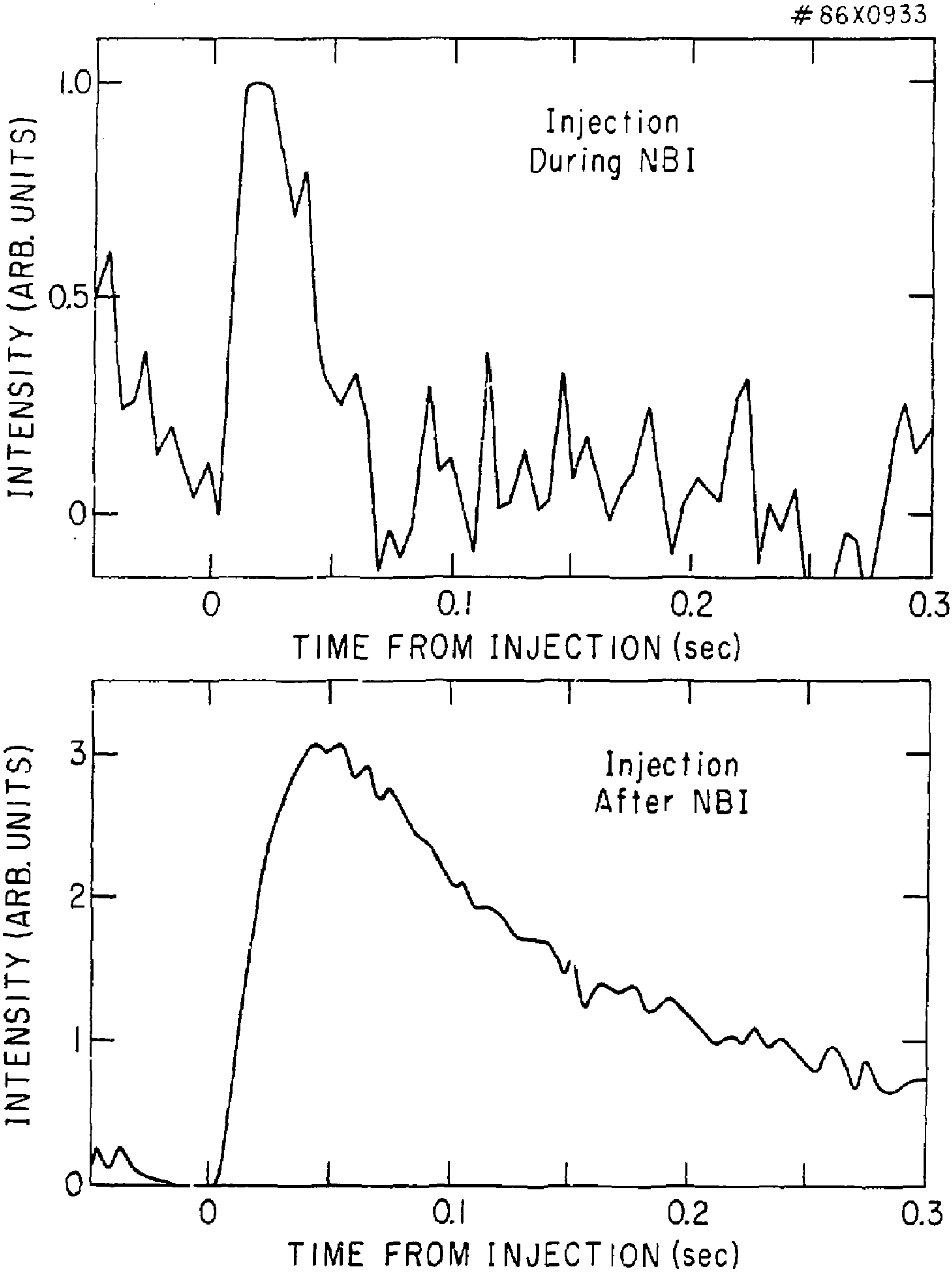
#86X0933
INTENSITY (ARB. UNITS)
1.0
0.5
0
Injection
During NBI
0
0.1
0.2
0.3
TIME FROM INJECTION (sec)
INTENSITY (ARB. UNITS)
3
2
1
0
Injection
After NBI
0
0.1
0.2
0.3
TIME FROM INJECTION (sec)

Fig. 5

EXTERNAL DISTRIBUTION IN ADDITION TO UC-20

Plasma Res Lab, Austra Nat'l Univ, AUSTRALIA
Dr. Frank J. Paoloni, Univ of Wollongong, AUSTRALIA
Prof. I.R. Jones, Flinders Univ., AUSTRALIA
Prof. M.H. Brennan, Univ Sydney, AUSTRALIA
Prof. F. Cap, Inst Theo Phys, AUSTRIA
M. Goossens, Astronomisch Instituut, BELGIUM
Prof. R. Boucique, Laboratorium voor Natuurkunde, BELGIUM
Dr. D. Palumbo, Dg XII Fusion Prog, BELGIUM
Ecole Royale Militaire, Lab de Phys Plasmas, BELGIUM
Dr. P.H. Sakanaka, Univ Estadual, BRAZIL
Lib. & Doc. Div., Instituto de Pesquisas Espaciais, BRAZIL
Dr. C.R. James, Univ of Alberta, CANADA
Prof. J. Teichmann, Univ of Montreal, CANADA
Dr. H.M. Skarsgard, Univ of Saskatchewan, CANADA
Prof. S.R. Sreenivasan, University of Calgary, CANADA
Prof. Tudor W. Johnston, INRS-Energie, CANADA
Dr. Hannes Barnard, Univ British Columbia, CANADA
Dr. M.P. Bachynski, MPB Technologies, Inc., CANADA
Chalk River, Nucl Lab, CANADA
Zhengwu Li, SW Inst Physics, CHINA
Library, Tsing Hua University, CHINA
Librarian, Institute of Physics, CHINA
Inst Plasma Phys, Academia Sinica, CHINA
Dr. Peter Lukac, Komenskeho Univ, CZECHOSLOVAKIA
The Librarian, Culham Laboratory, ENGLAND
Prof. Schatzman, Observatoire de Nice, FRANCE
J. Radet, CEN-BP6, FRANCE
JET Reading Room, JET Joint Undertaking, ENGLAND
AM Dupas Library, AM Dupas Library, FRANCE
Dr. Tom Mual, Academy Bibliographic, HONG KONG
Preprint Library, Cent Res Inst Phys, HUNGARY
Dr. R.K. Chhajlani, Vikram Univ, INDIA
Dr. B. Dasgupta, Saha Inst, INDIA
Dr. P. Kaw, Physical Research Lab, INDIA
Dr. Phillip Rosenau, Israel Inst Tech, ISRAEL
Prof. S. Cuperman, Tel Aviv University, ISRAEL
Prof. G. Rostagni, Univ Di Padova, ITALY
Librarian, Int'l Ctr Theo Phys, ITALY
Miss Clelia De Palo, Assoc EURATOM-ENEA, ITALY
Biblioteca, del CNR EURATOM, ITALY
Dr. H. Yamato, Toshiba Res & Dev, JAPAN
Direc. Dept. Lg. Tokamak Dev. JAERI, JAPAN
Prof. Nobuyuki Inoue, University of Tokyo, JAPAN
Research Info Center, Nagoya University, JAPAN
Prof. Kyoji Nishikawa, Univ of Hiroshima, JAPAN
Prof. Sigeru Mori, JAERI, JAPAN
Prof. S. Tanaka, Kyoto University, JAPAN
Library, Kyoto University, JAPAN
Prof. Ichiro Kawakami, Nihon Univ, JAPAN
Prof. Satoshi Itoh, Kyushu University, JAPAN
Dr. D.I. Choi, Adv. Inst Sci & Tech, KOREA
Tech Info Division, KAERI, KOREA
Bibliotheek, Fom-Inst Voor Plasma, NETHERLANDS
Prof. B.S. Liley, University of Waikato, NEW ZEALAND
Prof. J.A.C. Cabral, Inst Superior Tecn, PORTUGAL
Dr. Octavian Petrus, ALI CUZA University, ROMANIA
Prof. M.A. Hellberg, University of Natal, SO AFRICA
Dr. Johan de Villiers, Plasma Physics, Nucor, SO AFRICA
Fusion Div. Library, JEN, SPAIN
Prof. Hans Wilhelmson, Chalmers Univ Tech, SWEDEN
Dr. Lennart Stenflo, University of UMEA, SWEDEN
Library, Royal Inst Tech, SWEDEN
Centre de Recherchesen, Ecole Polytech Fed, SWITZERLAND
Dr. V.T. Tolok, Kharkov Phys Tech Ins, USSR
Dr. D.D. Ryutov, Siberian Acad Sci, USSR
Dr. G.A. Eliseev, Kurchatov Institute, USSR
Dr. V.A. Glukhikh, Inst Electro-Physical, USSR
Institute Gen. Physics, USSR
Prof. T.J.M. Boyd, Univ College N Wales, WALES
Dr. K. Schindler, Ruhr Universität, W. GERMANY
ASDEX Reading Rm, IPP/Max-Planck-Institut fur Plasmaphysik, F.R.G.
Nuclear Res Estab, Julich Ltd, W. GERMANY
Librarian, Max-Planck Institut, W. GERMANY
Bibliothek, Inst Plasmaforschung, W. GERMANY
Prof. R.K. Janev, Inst Phys, YUGOSLAVIA